J. Mater. Environ. Sci. 5 (6) (2014) 1988-1993
ISSN : 2028-2508
CODEN: JMESCN

Effect of partitioning time on microstructural evolution of a C-Mn-Si steel in two-step quenching and partitioning process

H.R. Ghazvinloo*, A. Honarbakhsh-Raouf
Department of Materials Engineering, Semnan University, Semnan, Iran.

Received 30 June 2014; Revised 25 July 2014; Accepted 25 July 2014.
**Corresponding Author. E-mail: Hamid.Ghazvinloo@Gmail.Com; Tel: (+982333484586)*

Abstract
Recently, quenching and partitioning as a new heat treatment process for producing steel microstructures containing carbon-enriched retained austenite proposed by Speer et al. This treatment includes full or partial austenitizing then quenching below the martensite start temperature (Ms) and in continue a partitioning step in same quenching temperature (one-step quenching and partitioning) or in a temperature above of quenching temperature (two-step quenching and partitioning). Austenitizing conditions, quenching temperature, partitioning time and temperature are the important parameters for this heat treatment. The present work focuses on effect of partitioning time on microstructural evolution in a C-Mn-Si steel during two-step quenching and partitioning process. For this aim, after full austenitization at 900 ^{0}C, samples were quenched into an oil bath at 238 ^{0}C and held for 10 s, then partitioned at 400 ^{0}C in a molten salt bath for times of 10, 30, 100, 400, 700 and 1000 s, finally water quenched to room temperature. After finishing heat treatments, the resulted multiphase microstructures were evaluated by optical microscopy and scanning electron microscopy, and the retained austenite volume fraction and its average carbon content were measured by X-ray diffraction method in heat treated samples.

Keywords: Two-step quenching and partitioning, partitioning time, microstructure, retained austenite.

1. Introduction
Recently, the need to develop advanced high strength steel (AHSS) with a range of properties that give engineers more flexibility in selecting an ideal grade of steel for any given application has raised increasing interest in developing a third generation of AHSS. The design of the 3rd generation of AHSS is intended to produce steels with a better combination of strength and ductility than the 1st generation of AHSS and at a lower cost than the 2nd generation of AHSS [1]. A key process for obtaining the 3rd generation AHSS is quenching and partitioning (Q&P) process which recently proposed by Speer et al. [2-7]. The heat treatment sequence involves quenching to a temperature between the martensite-start (M_s) and martensite-finish (M_f) temperatures, followed by a 'partitioning' treatment either at, or above, the initial quench temperature, designed to enrich the remaining untransformed austenite with carbon, escaping from the supersaturated martensite phase, thereby stabilizing retained austenite phase to room temperature [7]. Consequently, the final microstructure contains ferrite (in the case of partial austenitization), martensite and retained austenite.
Under the condition that partitioning is carried out at the quenching temperature, the process is named "one-step" Q&P process while "two-step" process involves reheating to a selected partitioning temperature that differs from the quenching temperature [8,9]. Microstructures obtained via Q&P process can lead to interesting mechanical properties [4,10], including a good formability and higher strength than conventional TRIP steels. So far few reports on microstructure characteristics of steels treated by Q&P process have been reported [11,12]. Therefore, the microstructural evolution of a C-Mn-Si steel treated by two-step Q&P process was investigated in this study.

2. Materials and methods
2.1. Materials
The chemical composition of the investigated material in this study has been shown in Table 1. 1.24 wt.% manganese was included in the chemical composition to retard ferrite, pearlite and bainite formation and to

decrease the bainite start temperature, as well as to enhance the austenite stability and a silicon content of 1.38 wt.% was used to restrict carbide precipitation during the partitioning step [13].

Table 1: The chemical composition of the investigated material (wt.%)

C	0.362	Mo	0.005
Si	1.38	Ni	0.0902
Mn	1.24	Al	0.03
P	0.0245	Co	0.0101
S	0.0202	Cu	0.0711
Cr	0.0973	B	0.002
Nb	0.0025	Ca	0.0008
Ti	0.0023	Zr	0.002
V	0.002	As	0.0101
W	0.015	Sn	0.0095
Pb	0.025	Fe	Base

2.2. Two-step Q&P heat treatment

For two-step Q&P heat treatment, the specimens were heated to 900 ^{0}C at heating rate of +5 ^{0}C/s in a furnace and held for 10 minutes for full austenitization in continue, quenched into an oil bath at 238 ^{0}C (optimum quenching temperature) with cooling rate of -220 ^{0}C/s and held for 10 s, then partitioned at 400 ^{0}C in a molten salt bath for times of 10, 30, 100, 400, 700 and 1000 s, finally water quenched to room temperature (Figure 1).

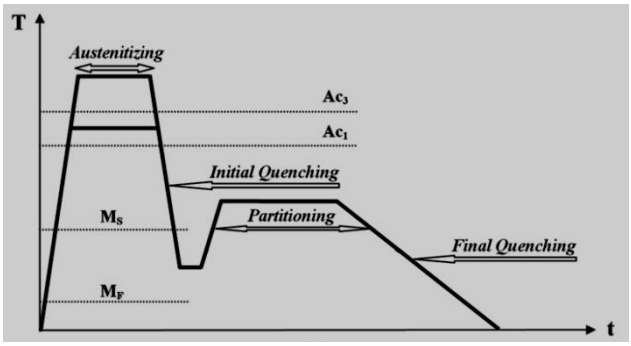

Figure 1: Schematic of two-step Q&P process applied in present work (M_S=339 ^{0}C, Ac_1=748.1 ^{0}C, Ac_3=841.5 ^{0}C).

2.3. Characterization

Having finished the heat treatments, the treated samples were ground and polished mechanically then etched with 2% nital for 6-8 s. After conventional metallographic preparation, the microstructural examination of the samples was conducted using optical microscopy and JEOL JXA-840 SEM. In order to determine the retained austenite volume fraction and its average carbon content in the specimens treated by two-step Q&P process, X-ray diffraction (XRD) measurements were performed on a Bruker D8 diffractometer using CuKα radiation operating at 35 kV and 30 mA. Samples were scanned over a 2θ range from 10 to 90 deg with a dwelling time of 1s and a step size of 0.05 deg. The volume fraction of retained austenite was measured based on the direct comparison method [14] by using the integrated intensity of the $(200)_\gamma$, $(220)_\gamma$; $(200)_M$, $(211)_M$ peaks and the average carbon content of retained austenite was measured according to following equation [15]. The average carbon content obtained from both austenite peak positions was calculated [16] in this study.

$$a_0 = 3.555 + 0.044x$$

Where a_0 is austenite lattice parameter in angstroms and x is average carbon content of austenite in weight percent.

3. Results and discussion

3.1. Optical microscopy observations

Optical micrographs showing the morphology of the specimens treated by two-step Q&P process with partitioning times of 10, 100, and 1000 s have been shown in Figure 2. According to it, a mixture of martensite and carbon-enriched retained austenite phases was separably observed in the all specimens

partitioned for different times. Moreover, bainite phase was detected in microstructure of samples treated at longer partitioning times (arriving to bainite region has not probably been possible in shorter partitioning times). Base on Koistinen–Marburger relationship (following equation) [17], the volume fraction of virgin martensite and untransformed austenite after quenching at 238 ^{0}C and prior to partitioning process were approximately predicted 67 and 33 vol pct.

$$f_m = 1 - e^{-0.011(M_s - QT)}$$

where M_s is martensite start temperature, QT is quenching temperature and f_m is volume fraction of martensite produced in quenching temperature (QT). Since, the carbon content of steel used in this study was less than 0.6 wt.%; hence, the virgin martensite has had a lath morphology.
After the second quenching to room temperature, a proportion of untransformed austenite with enough carbon content could be stabilized at room temperature, another proportion of untransformed austenite with a carbon content enough high transformed into twin martensite and the rest of the untransformed austenite with a lower carbon content transformed into plate or lath martensite at room temperature [18].

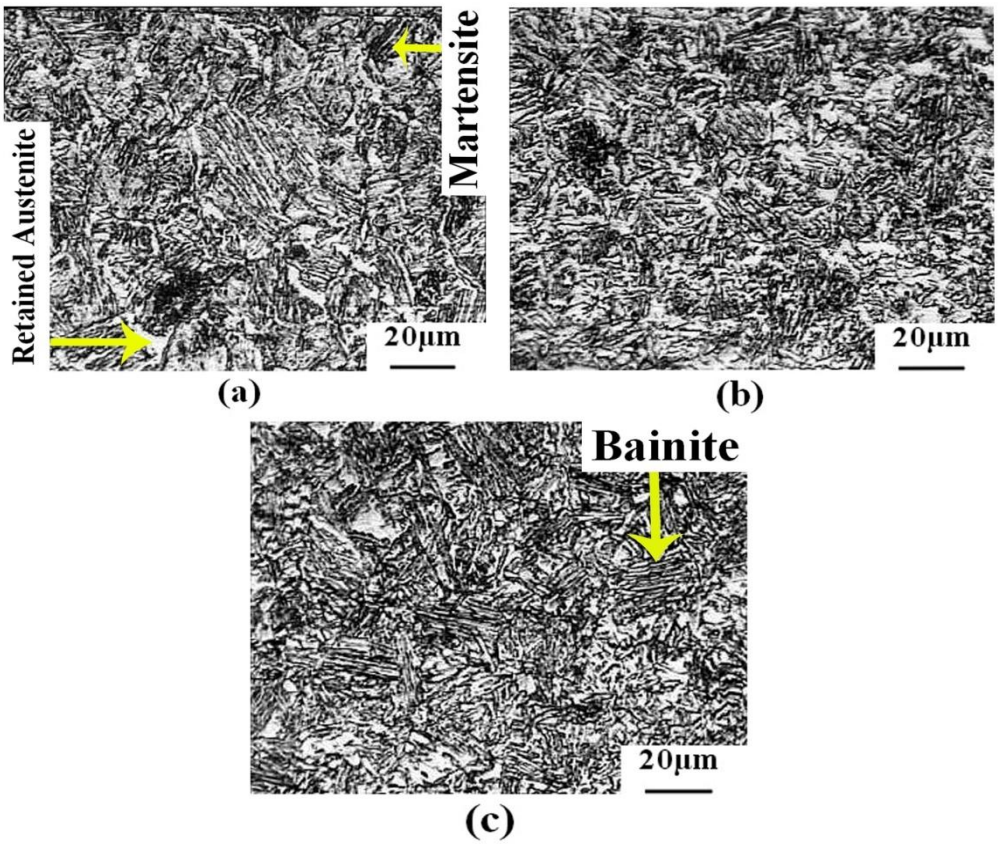

Figure 2: Optical micrographs for treated specimens: full austenitized at 900 ^{0}C, quenched to 238 ^{0}C, partitioned at 400 ^{0}C for (a)10 (b)100 and (c)1000 s, finally water quenched to room temperature.
Optical microscopy observations give indications about the microstructure present in the specimens for every Q&P condition. However, they do not provide microstructural details smaller than a few microns [19]; therefore, SEM was used for these purposes.

3.2. SEM observations
The SEM micrographs for treated specimens have been shown in Figure 3. According to it, there existed two kinds of retained austenite with different morphology and size. One was the island-like shape and distributed along the grain boundary mainly, and a few of them distributed within martensite matrix; the other was the film-like shape and distributed between martensite laths [20]. Cementite carbide (Fe_3C) precipitation was observed in specimens partitioned for 30 s and, bainite phase was detected in microstructure of samples treated at 400, 700 and 1000 s.

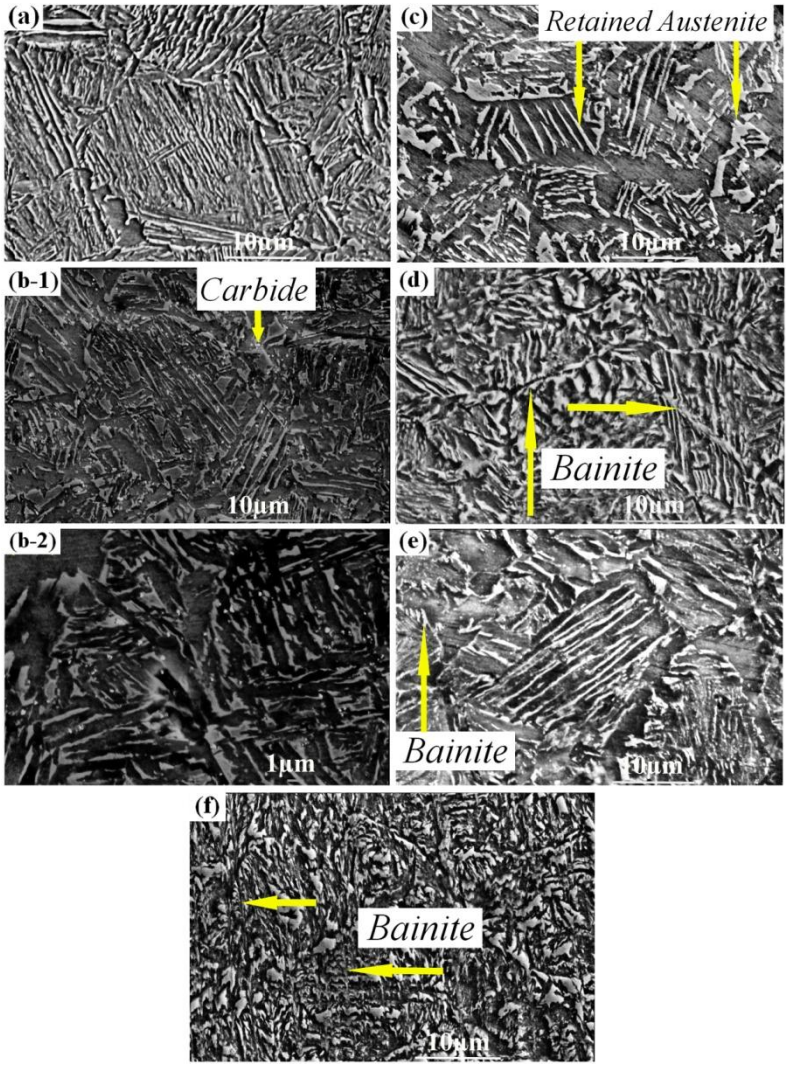

Figure 3: SEM micrographs for treated specimens: full austenitized at 900 ^{0}C, quenched to 238 ^{0}C, partitioned at 400 ^{0}C for (a)10 (b)30 (c)100 (d)400 (e)700 (f)1000 s, finally water quenched to room temperature.

3.3. XRD Analysis

The average carbon content measured for different partitioning times has been shown in Figure 4.

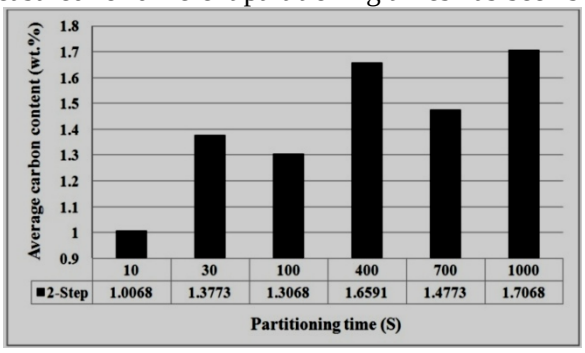

Figure 4: The average carbon content of retained austenite measured for different partitioning times.

The least average carbon content was 1.0068% which obtained at partitioning time of 10 s and it may be due to diffusion of a few carbon atoms from supersaturated martensite to untransformed austenite during 10 s of partitioning. The occurrence of carbide precipitation was observed in sample partitioned for 30 s, but the diffusion of carbon was a dominant process at this partitioning time and leaded to an increasing in the average carbon content of retained austenite to 1.3773%. The average carbon content of retained austenite decreased to 1.3068% in specimen partitioned for 100 s. It can be due to processes related with the conventional martensite

tempering, like carbon segregation in martensite. It can reduce the amount of carbon available for the enrichment of the austenite during the partitioning step [21]. In continue the average carbon content of retained austenite increased intensively to 1.6591% in specimen partitioned for 400 s and its amount was retained in high levels (1.4773% and 1.7068%) in specimens partitioned for 700 and 1000 s. It can be due to bainite phase formation in microstructure of specimens partitioned at 400, 700 and 1000 s. Adding to partitioning of carbon to untransformed austenite from carbon supersaturated martensite, carbon enrichment of austenite associated with the formation of carbide-free bainite, especially in any large austenite pools is noteworthy in Q&P processes [22].

Retained austenite plays the key role on plasticity enhancement. As been pointed out in Ref. [23], interlath film-like austenite can impede generation and propagation of cracks and in turn improve toughness effectively; Furthermore, both interlath and island-like austenite can partially transform to martensite and show 'TRIP' effect during deformation, eliminating stress concentration and retarding the happening of necking [24], which results in the increasing of both strength and elongation. The retained austenite volume fraction measured for different partitioning times has been shown in Figure 5. Also, XRD patterns of steel treated by two-step Q&P process with the greatest and least volume fraction of retained austenite have been shown in Figure 6. With increasing in average carbon content of untransformed austenite during partitioning stage, its M_s temperature decreases and its thermal stability increases. Therefore, carbon enrichment of untransformed austenite with partitioning process will increase the volume fraction of retained austenite. The least volume fraction of retained austenite was 9.08% which obtained at partitioning time of 10 and 700 s and it was due to low average carbon content of untransformed austenite in specimen partitioned at 10 s. Increasing of average carbon content of untransformed austenite in specimen partitioned at 30 s leaded to increase the retained austenite volume fraction from 9.08 to 12.35%. The higher homogeny in distribution of diffusing carbon atoms within untransformed austenite at partitioning time of 100 s than 30 s, resulted in a maximum volume fraction of retained austenite in this condition (13.58%). But decreasing in retained austenite volume fraction in specimens treated at partitioning times of 400, 700 and 1000 s can be due to bainite phase formation in these conditions. If bainite formation be able to occur during partitioning, then austenite present at the QT may be consumed, reducing the capacity for austenite stabilization through the proposed partitioning mechanism [25].

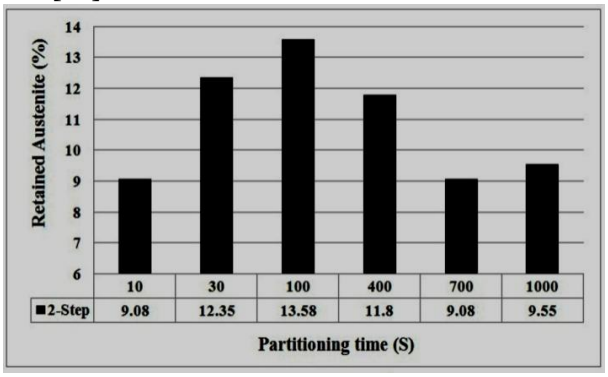

Figure 5: The retained austenite volume fraction measured for different partitioning times.

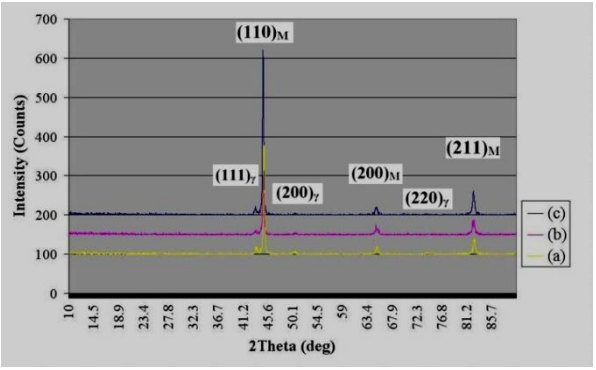

Figure 6: XRD patterns for steel treated by two-step Q&P process with (a) maximum and (b),(c) minimum volume fraction of retained austenite.

Conclusion

Two kinds of retained austenite with different morphology and size were observable in heat treated specimens. One was the island-like shape and distributed along the grain boundary mainly, and a few of them distributed within martensite matrix; the other was the film-like shape and distributed between martensite laths. Carbide precipitation occurrence was observed in specimen partitioned at 30 s and bainite phase formation was observed in specimens partitioned at 400, 700 and 1000 s. Occurance of carbide formation reduce the average carbon content of retained austenite whereas, bainite formation increase average carbon content of retained austenite and reduce volume fraction of retained austenite. With increasing of average carbon content of untransformed austenite during partitioning stage, its M_s temperature decreases and its thermal stability increases. Therefore, carbon enrichment of untransformed austenite with partitioning process will increase the volume fraction of retained austenite. In this study, the maximum average carbon content of retained austenite was 1.7068% which obtained at partitioning time of 1000 s and the greatest volume fraction of retained austenite was 13.58% which obtained at partitioning time of 100 s.

Acknowledgements-The authors would like to thank of Dr. Ali Reza Kiani Rashid for his assistance in the preparation of this article and, Oghabafshan Industrial & Manufacturing Company and Semnan University for all the facilities.

References

1. Qu H., Master of Science Thesis, Department of Materials Science and Engineering, Case Western Reserve University (2011).
2. Matlock D. K., Bräutigam V. E., Speer J. G., *Mater. Sci. Forum.* 426–432 (2003) 1089.
3. Speer J. G., Matlock D. K., De Cooman B. C., Schroth J. G., *Acta Mater*. 51 (2003) 2611.
4. Speer J. G., Edmonds D. V., Rizzo F. C., Matlock D. K., *Curr. Opin. Solid State Mater. Sci.* 8 (2004) 219.
5. Clarke A. J., Speer J. G., Matlock D. K., Rizzo F. C., *Scr. Mater.* 61 (2009) 149.
6. Streicher A. M., Speer J. G., Matlock D. K., De Cooman B. C., Proceedings of the international conference on advanced high strength sheet steels for automotive applications, (2004) Warrendale, PA: AIST.
7. Edmonds D. V., He K., Rizzo F. C., De Cooman B. C., Matlock D. K., Speer J. G., *Mater. Sci. Eng. A.* 438-440 (2006) 25.
8. Speer J. G., Matlock D. K., De Cooman B. C., Schroth J. G., *Acta Mater.* 51 (2003) 2611.
9. Zu-yao XU, New Processes for Steel Heat Treatment [J]. Heat Treatment, 22, (2007).
10. Edmonds D. V., He K., Rizzo F. C., Clarke A. M. S., Matlock D. K., Speer J. G., 1st Int. Conf. on Super High Strength Steels, (2005); Rome, Italy.
11. Santofimia M. J., Zhao L., Petrov R., Sietsma J., *Mater. Charact.* 59 (2008) 1758.
12. Santofimia M. J., Zhao L., Sietsma J., *Metall. Mat. Trans. A.* 40A (2009) 46.
13. Santofimia M. J., Zhao L., Petrov R., Kwakernaak C., Sloof W. G., Sietsma J., *Acta Mater.* 59 (2011) 6059.
14. Cullity B. D., Stock S. R., Elements of X-ray Diffraction, 3rd ed., Prentice Hall, New York (2001).
15. Cullity B. B., Elements of X-Ray Diffraction, 2nd ed., Addison-Wesley Publishing Co., Inc. (1978).
16. De Moor E., Lacroix S., Clarke A. J., Penning J., Speer J. G., *Metall. Mater. Trans. A*. 39A (2008) 2586.
17. Krauss G., STEELS: Heat treatment and processing principles, ASM International, Second Edition (1990).
18. Li H. Y., Lu X. W., Li W. J., Jin X. J., *Metall. Mater. Trans. A.* 41A (2010) 1284.
19. Santofimia M. J., Zhao L., Sietsma J., *Metall. Mater. Trans. A.* 40A (2009) 46.
20. Wang X. D., Guo Z. H., Rong Y. H., *Mater. Sci. Eng. A.* 529 (2011) 35.
21. Santofimia M. J., Zhao L., Petrov R., Sietsma J., *Mater. Charac.* 59 (2008) 1758.
22. Clarke A. J., Speer J. G., Miller M. K., Hackenberg R. E., Edmonds D. V., Matlock D. K., Rizzo F. C., Clarke K. D., De Moor E., *Acta Mater.* 56 (2008) 16.
23. Rao B. V. N., Thomas G., *Metall. Trans.* A. 11 (1980) 441.
24. Wang X. D., Huang B. X., Rong Y. H., Wang L., *J. Mater. Sci. Technol.* 22 (2006) 625.
25. De Moor E., Lacroix S., Clarke A. J., Penning J., Speer J. G., *Metall. Mater. Trans. A.* 39A (2008) 2586.